Electronic Supplementary Material (ESI) for Nanoscale.

Electronic Supplementary Information (ESI) for

Preparation of polymer nanocomposite via the polymerization of pyrrole:biphenyldisulfonic acid:pyrrole as two-monomer-connected precursor on MoS_2 for electrochemical energy storage

Wonbin Kim,[a] Hong-Joon Lee,[a] Seung Jo Yoo,[b] Cuc Kim Trinh,[a] Zubair Ahmad[a] and Jae-Suk Lee*[a]

[a]School of Materials Science and Engineering, Gwangju Institute of Science and Technology (GIST), 123 Cheomdangwagi-ro, Buk-gu, Gwangju 61005, Korea
[b]Center of Research Equipment, Korea Basic Science Institute (KBSI), 169-148 Gwahak-ro, Yuseong-gu, Daejeon 34133, Korea.

*Corresponding Author. E-mail: jslee@gist.ac.kr

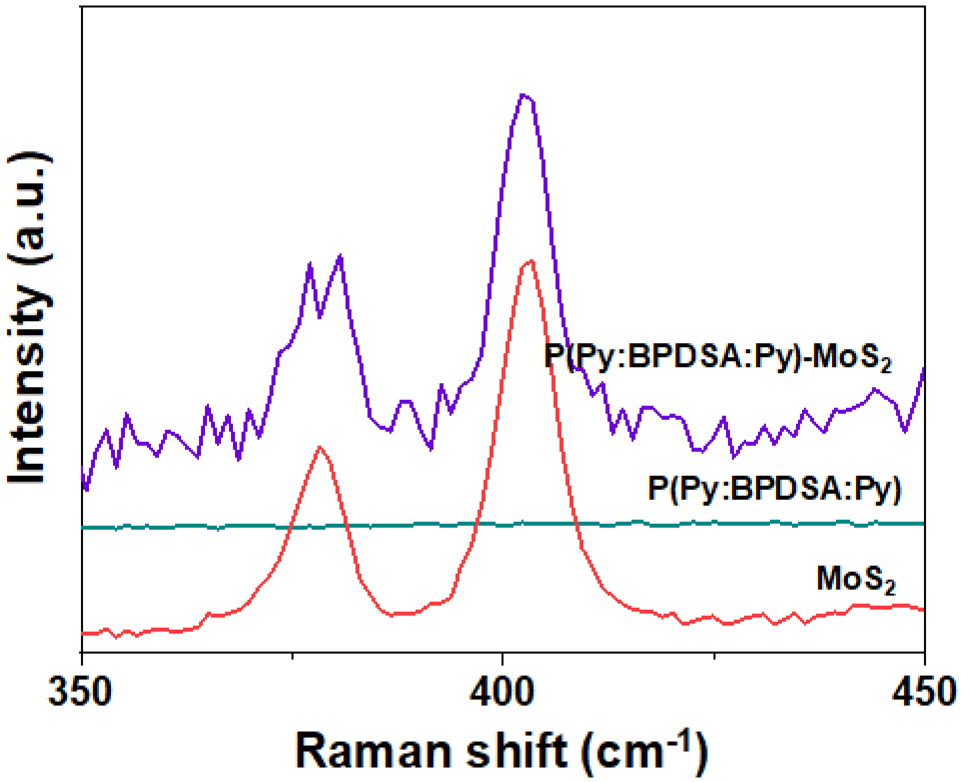

Fig. S1 Raman spectroscopy of P(Py:BPDSA:Py)-MoS_2 (MoS_2 50%), P(Py:BPDSA:Py) and MoS_2, range from 350 to 450 cm^{-1}.

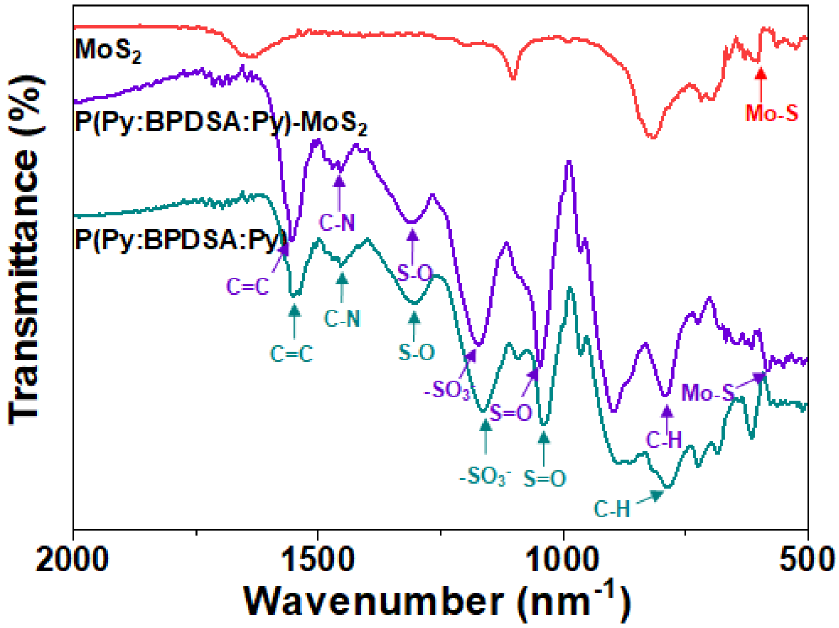

Fig. S2 FT-IR spectroscopy of P(Py:BPDSA:Py)-MoS_2 (MoS_2 50%), P(Py:BPDSA:Py) and MoS_2. range from 500 to 2000 nm^{-1}. Most of the characterisic peaks related to the polymer, P(Py:BPDSA:Py), were shifted in the composite, P(Py:BPDSA:Py)-MoS_2, demonstrating the Interaction between the MoS_2 and polymer. In the spectra of P(Py:BPDSA:Py)-MoS_2, the characterisic peaks of P(Py:BPDSA:Py) were observed and shifted from 1546 (C=C), 1455 (C-N), 1303 (S-O), 1164 (-SO_3), 1039 (S=O), 788 nm^{-1} (C-H) to 1552 (C=C), 1463 (C-N), 1311 (S-O), 1174 (-SO_3), 1049 (S=O), 794 nm^{-1} (C-H).[1-3] The Mo-S vibration peak associated with MoS_2 was also observed at about 600 nm^{-1} in the P(Py:BPDSA:Py)-MoS_2.[4-6]

1. H. Tang, J. Wang, H. Yin, H. Zhao, D. Wang and Z. Tang, *Adv. Mater.*, 2015, **27**, 1117-1123.

2. H.-J. Lee, Y.-R. Jo, S. Kumar, S. J. Yoo, J.-G. Kim, Y.-J. Kim, B.-J. Kim and J.-S. Lee, *Nat. Commun.*, 2016, **7**, 1-6.

3. R. Zeng, Z. Li, L. Li, Y. Li, J. Huang, Y. Xiao, K. Yuan and Y. Chen, *ACS Sustainable Chem. Eng.*, 2019, **7**, 11540-11549.

4. N. Maity, A. Mandal and A. K. Nandi, *J. Mater. Chem. C*, 2017, **5**, 12121-12133.

5. S. S. Karade, D. P. Dubal and B. R. Sankapal, *RSC Adv.*, 2016, **6**, 39159-39165.

6. Y. Chen, W. Ma, K. Cai, X. Yang and C. Huang, *Electrochim. Acta*, 2017, **246**, 615-624.

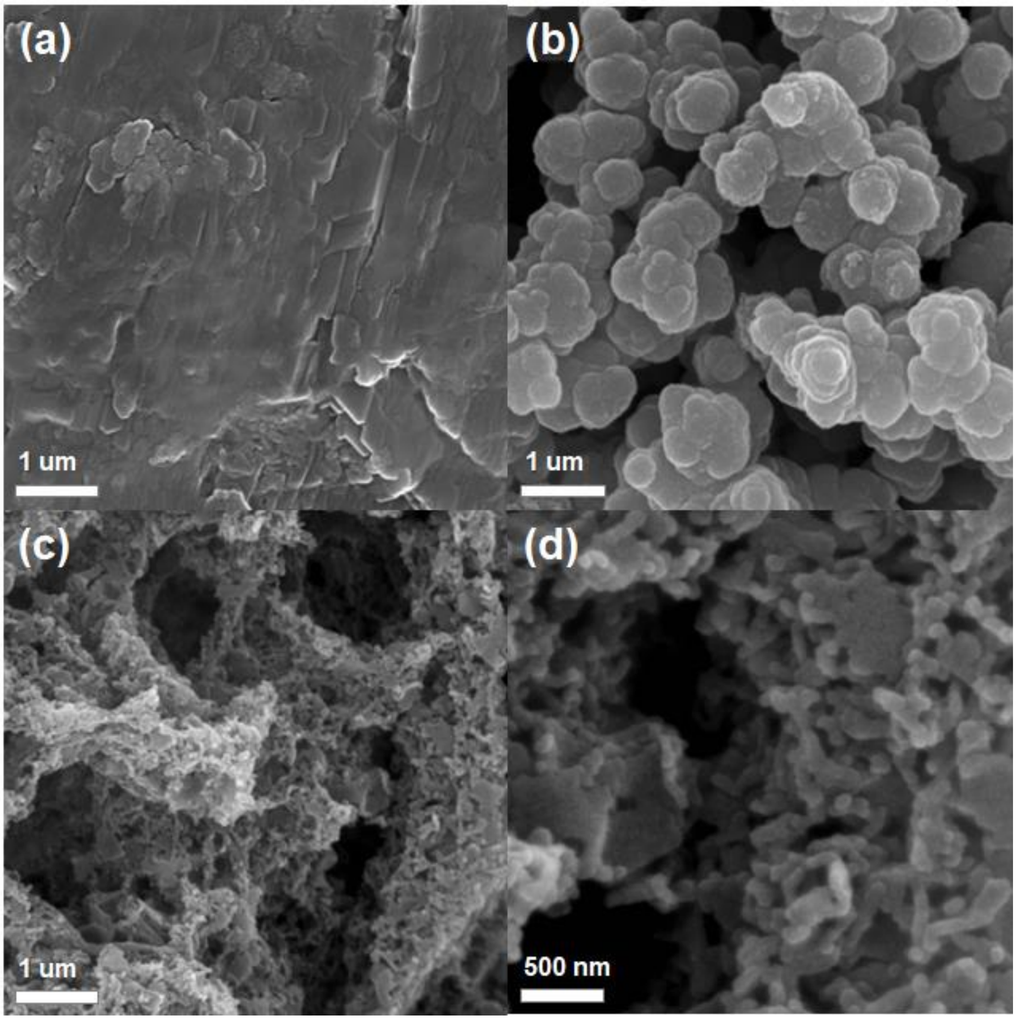

Fig. S3 SEM image of (a) MoS_2, (b) P(Py:BPDSA:Py), (c) P(Py:BPDSA:Py)-MoS_2 (MoS_2 50%). Scale bar, 1 μm. (d) P(Py:BPDSA:Py)-MoS_2 (MoS_2 50%). Scale bar, 500 nm.

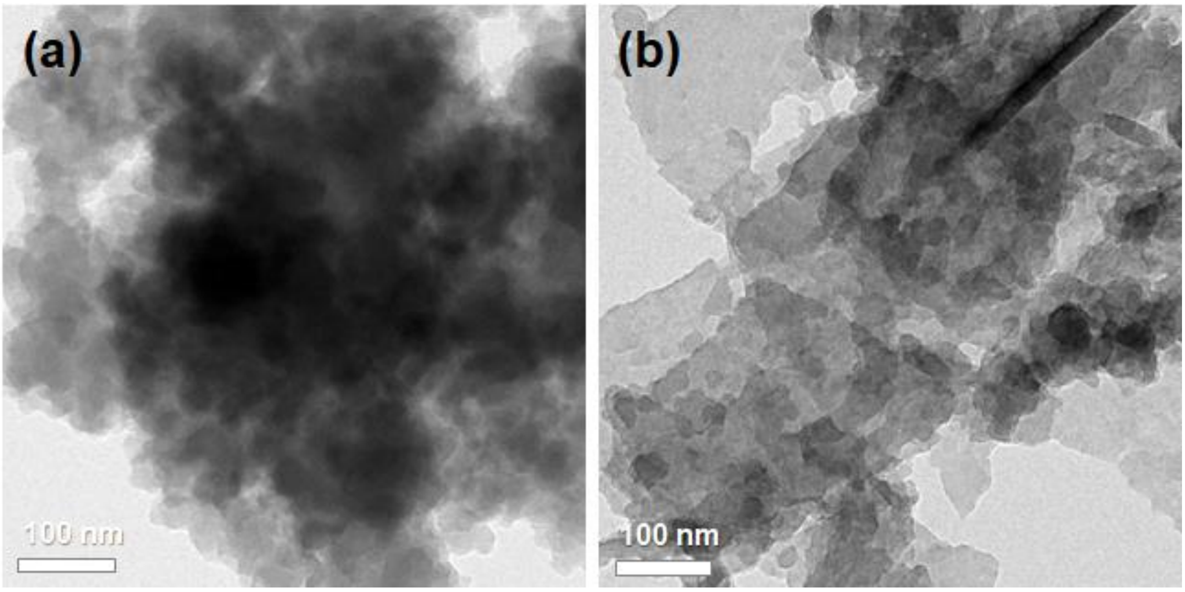

Fig. S4 TEM image of (a) P(Py:BPDSA:Py) and (b) P(Py:BPDSA:Py)-MoS_2 (MoS_2 50%).

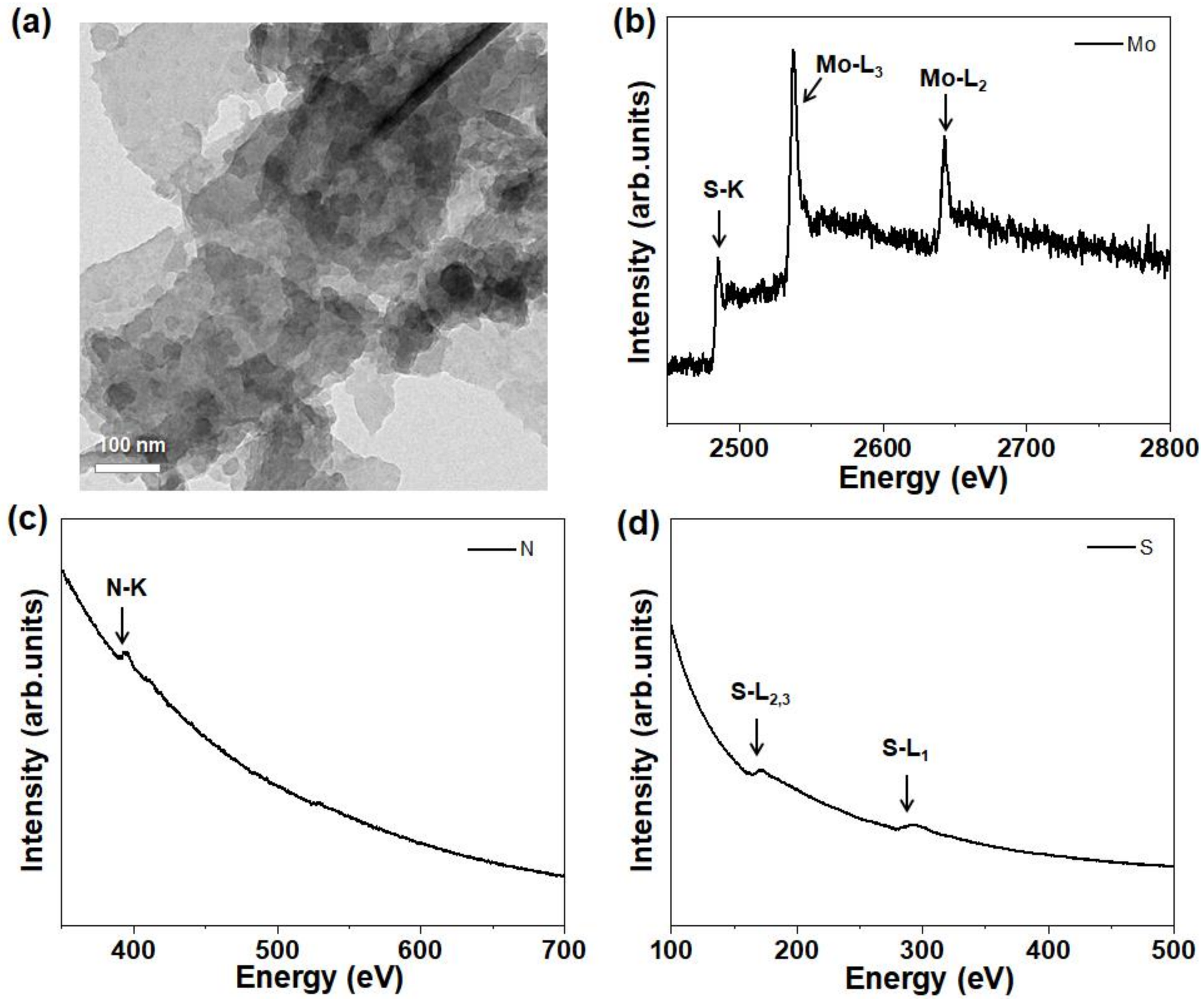

Fig. S5 (a) TEM image of P(Py:BPDSA:Py)-MoS_2 (MoS_2 50%). Electron energy loss spectroscopy (EELS)

P(Py:BPDSA:Py)-MoS_2 (MoS_2 50%), (b) Molybdenum (Mo), (c) Nitrogen (N), and (d) Sulfur (S).

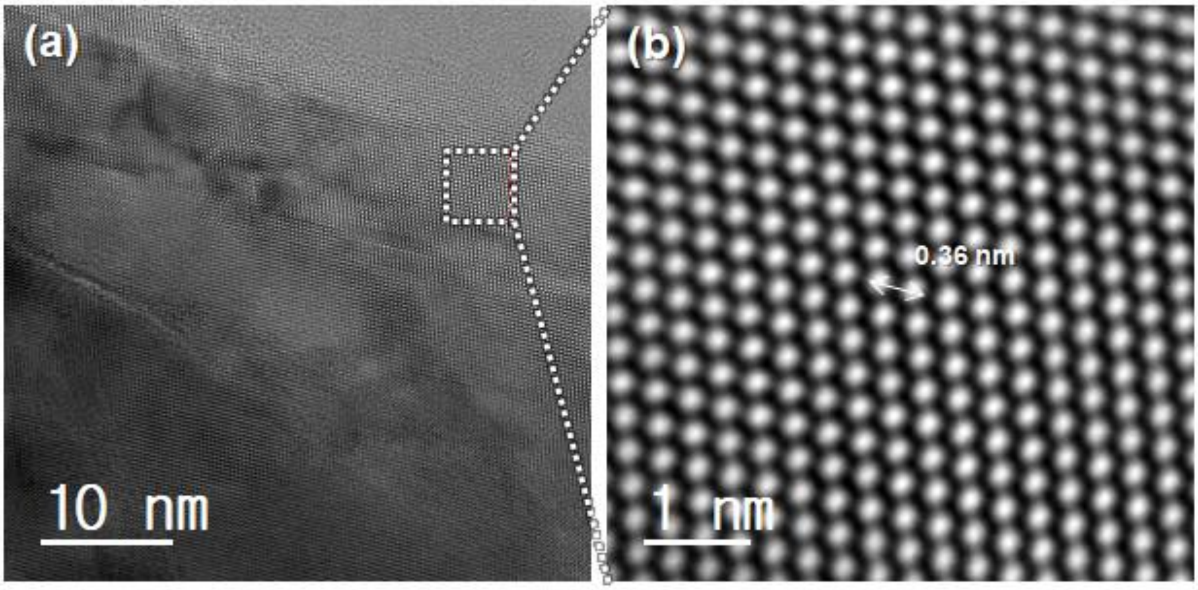

Fig. S6 Molecular-level ordering of P(Py:BPDSA:Py)-MoS_2 (MoS_2 50%). (a) HRTEM image measured along [011] zone axis, (b) Intensity profile of the lines for the white line covered area in figure (a). The fourth-order reflecti on (400) *d* spacing of 0.36 nm is observed in the [100] direction. This is similar to the *d* spacing of the polymer, P(Py:BPDSA:Py), crystal structure.[1]

1. H.-J. Lee, Y.-R. Jo, S. Kumar, S. J. Yoo, J.-G. Kim, Y.-J. Kim, B.-J. Kim and J.-S. Lee, *Nat. Commun.*, 2016, **7**, 1-6.

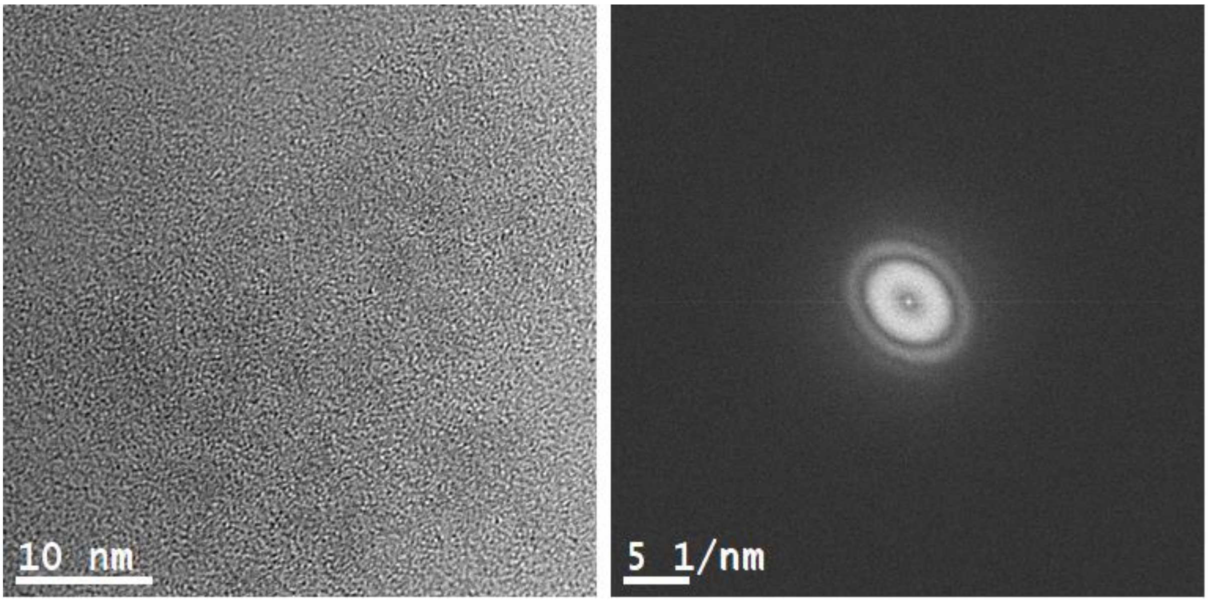

Fig. S7 HRTEM and FFT pattern image of P(Py:MSA)-MoS_2 (MoS_2 50%).

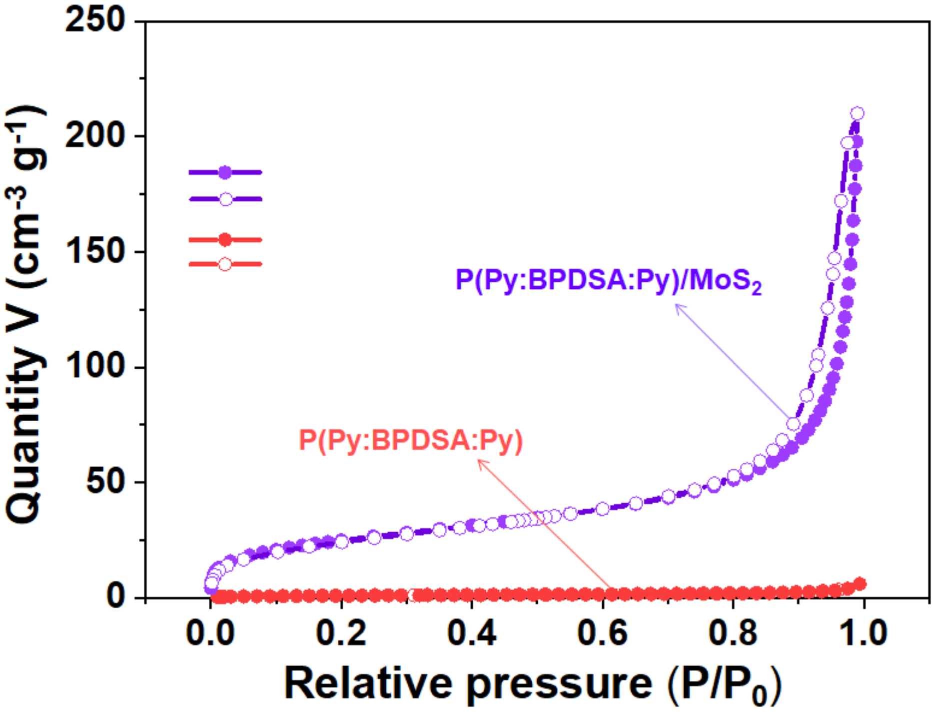

Fig. S8 N_2 adsorption/desorption isotherms of P(Py:BPDSA:Py) and P(Py:BPDSA:Py)-MoS_2 (MoS_2 50%).

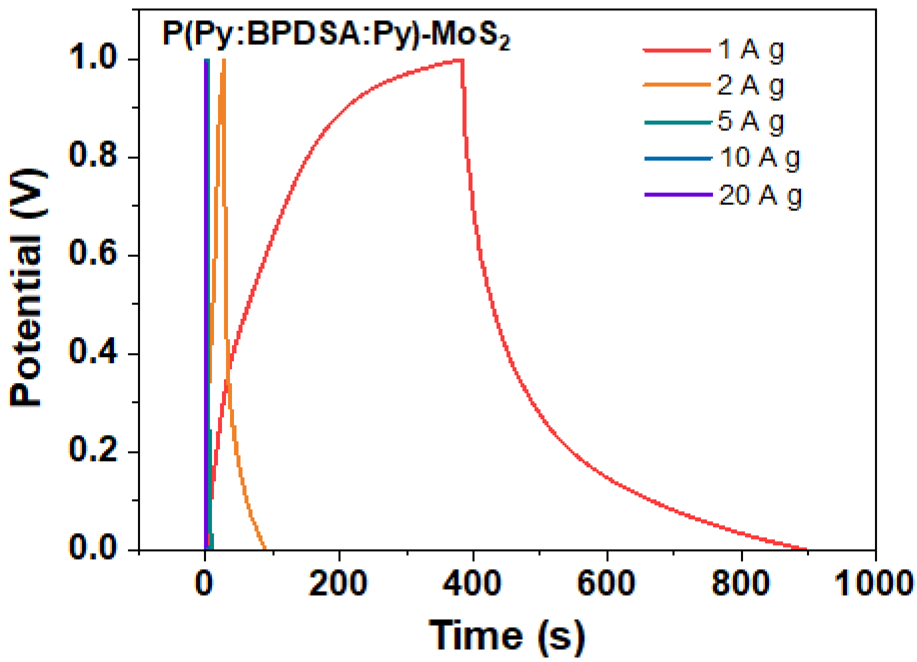

Fig. S9 Galvanostatic charge/discharge measurement of P(Py:BPDSA:Py)-MoS_2 (MoS_2 50%) at various current densities.

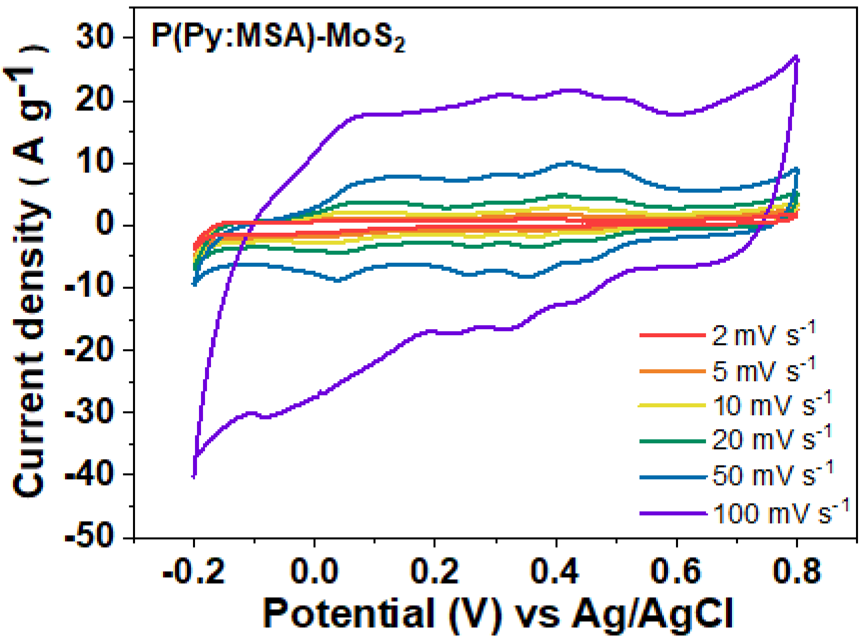

Fig. S10 CV curves of P(Py:MSA)-MoS_2 (MoS_2 50%) at various scan rates.

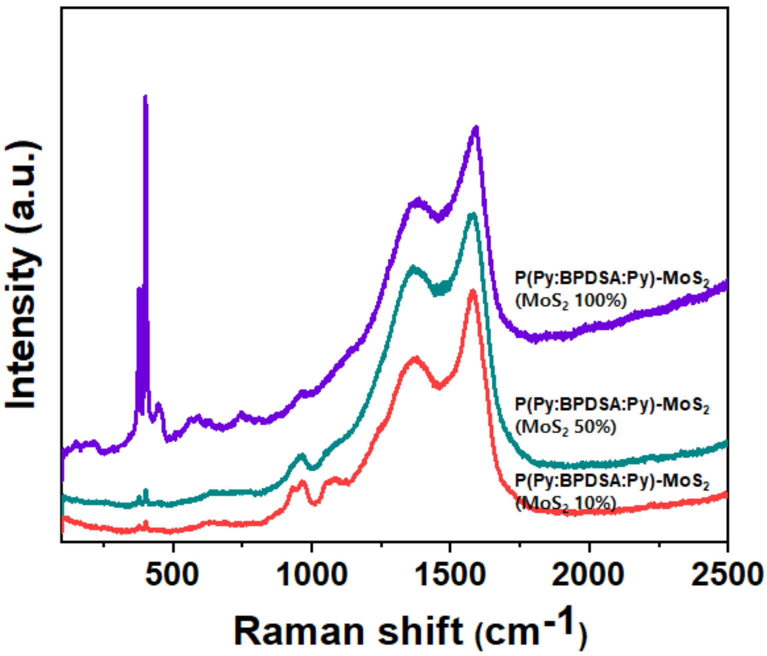

Fig. S11 Raman spectroscopy of composite, P(Py:BPDSA:Py)-MoS_2 (MoS_2 - 10, 50, 100%). The characteristic peak of MoS_2 appears stronger in the composite, P(Py:BPDSA:Py)-MoS_2 (MoS_2 100%).

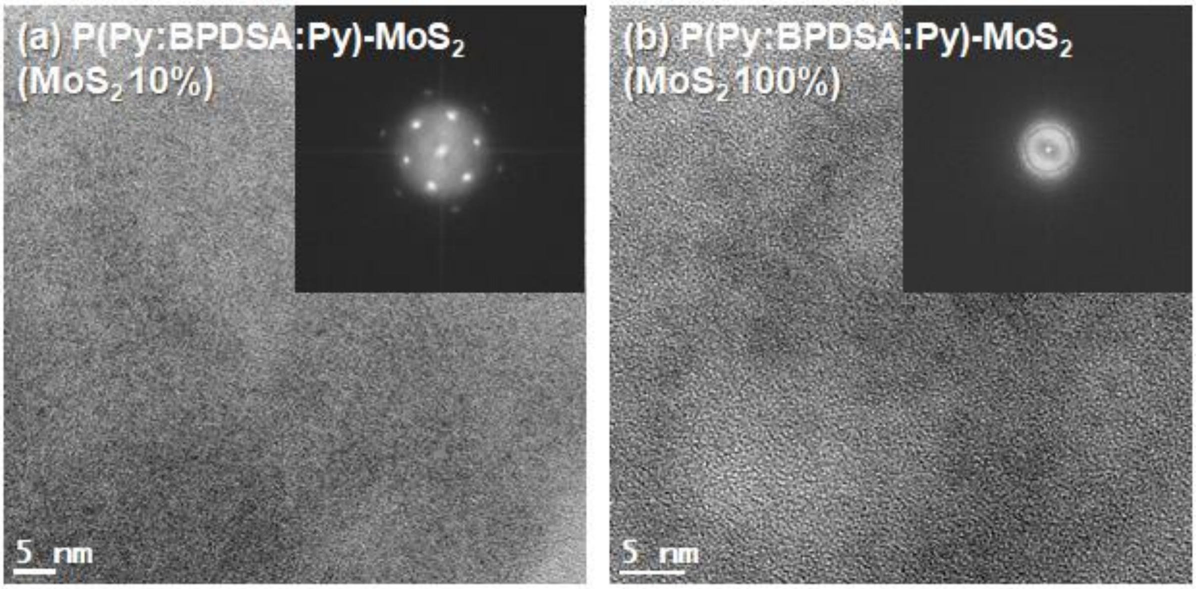

Fig. S12 HRTEM and processed FFT pattern images of P(Py:BPDSA:Py)-MoS_2 (MoS_2 - 10, 100%). As the mass of MoS_2 increases, the crystallinity of the composite decreases. It can be inferred that the increased MoS_2 monolayers may aggregate and interfere with the crystal growth of the polymer.

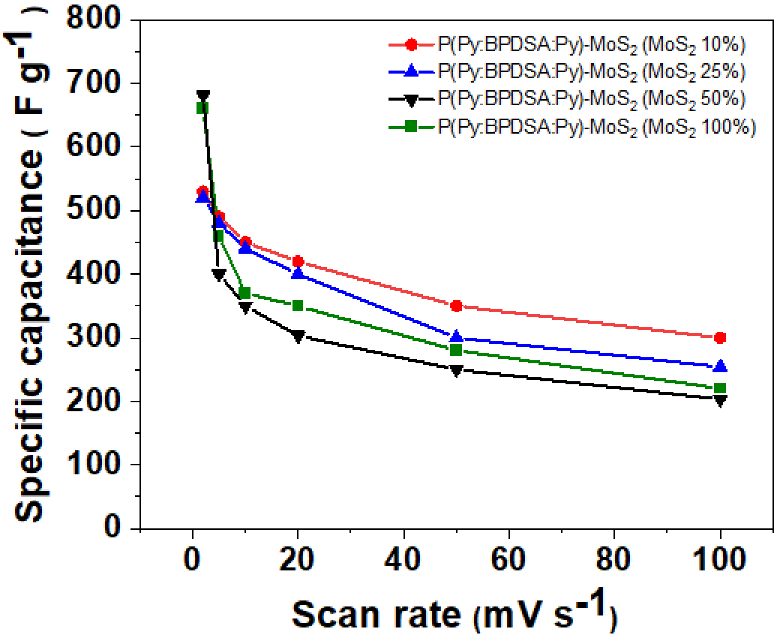

Fig. S13 Specific capacitances of composites, P(Py:BPDSA:Py)-MoS_2 (MoS_2 - 10, 25, 50, 100%), at various scan rates. As the mass of MoS_2 increases, the specific capacitances of the composite also increase at 2 mV s^{-1}, but the rate capability decreases. it can be inferred that if the crystalline polymer is simply increased, the polymer grows thickly on the MoS_2 even though the crystallinity of the composite increases, which leads to a decrease in the porosity and thus the ion mobility, but rate capability retains because polymer crystal effect to the stability.

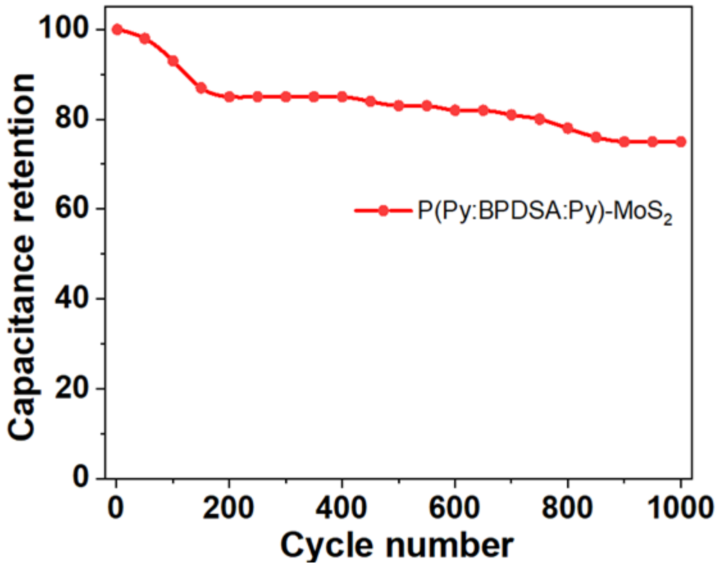

Fig. S14 Capacitance retention of composite, P(Py:BPDSA:Py)-MoS_2 (MoS_2 50%), at a scan rate of 10 mV s^{-1}

Table S1 The capacitances of the MoS_2 based materials reported in the literatures.

Electrode active material	Electrolyte	Scan rate or current density	Specific capacitance ($F\ g^{-1}$ or $F\ cm^{-3}$)	Reference
P(Py:BPDSA:Py)/MoS_2	1 M H_2SO_4	2 mV $s^{-1.}$	681 (3-electrodes)	This work
PPy/MoS_2	1 M KCl	0.5 A g^{-1}	695 (2-electrodes)	1
PPy/MoS_2	1 M KCl	1 A g^{-1}	554 (3-electrodes)	2
PPy/MoS_2	0.5 M Na_2SO_4	1 A g^{-1}	462 (3-electrodes)	3
PPy/MoS_2-DBS	1 M LiCl	0.5 mA/cm^2	325 (3-electrodes)	4
PANI/MoS_2	1 M H_2SO_4	1 A g^{-1}	575 (3-electrodes)	5
PANI/MoS_2	KOH	1 A g^{-1}	510.12 (3-electrodes)	6
PANI/MoS_2	0.5 M H_2SO_4	1 A g^{-1}	450 (3-electrodes)	7
PANI/MoS_2	1 M H_2SO_4	5 mV $s^{-1.}$	364 (3-electrodes)	8
PANI/MoS_2	1 M H_2SO_4	10 A g^{-1}	245.5 (3-electrodes)	9
PANI/MoS_2-NH_2	1 M H_2SO_4	0.5 A g^{-1}	326.4 (3-electrodes)	10
PANI/CNT/MoS_2	1 M H_2SO_4	1 A g^{-1}	350 (2-electrodes)	11
PEDOT/MoS_2	2 M HCl	5 mV $s^{-1.}$	452 (3-electrodes)	12

1. H. Tang, J. Wang, H. Yin, H. Zhao, D. Wang and Z. Tang, *Adv. Mater.*, 2015, **27**, 1117-1123.

2. G. Ma, H. Peng, J. Mu, H. Huang, X. Zhou and Z. Lei, *J. Power Sources*, 2013, **229**, 72-78.

3. Y. Chen, W. Ma, K. Cai, X. Yang and C. Huang, *Electrochim. Acta*, 2017, **246**, 615-624.

4. Y. Tian, J. Liu, X. Song, L. Zhao, P. Zhang and L. Gao, *Compos. Sci. Technol.*, 2020, **197**, 108263.

5. K.-J. Huang, L. Wang, Y.-J. Liu, H.-B. Wang, Y.-M. Liu and L.-L. Wang, *Electrochim. Acta*, 2013, **109**, 587-594.

6. S. A. Ansari, H. Fouad, S. Ansari, M. P. Sk and M. H. Cho, *J. Colloid Interface Sci.*, 2017, **504**, 276-282.

7. J. Lei, Z. Jiang, X. Lu, G. Nie and C. Wang, *Electrochim. Acta*, 2015, **176**, 149-155.

8. S. Zhang, X. Song, S. Liu, F. Sun, G. Liu and Z. Tan, *Electrochim. Acta*, 2019, **312**, 1-10.

9. J. Chao, J. Deng, W. Zhou, J. Liu, R. Hu, L. Yang, M. Zhu and O. G. Schmidt, *Electrochim. Acta*, 2017, **243**, 98-104.

10. R. Zeng, Z. Li, L. Li, Y. Li, J. Huang, Y. Xiao, K. Yuan and Y. Chen, *ACS Sustainable Chem. Eng.*, 2019, **7**, 11540-11549.

11. A. K. Thakur, A. B. Deshmukh, R. B. Choudhary, I. Karbhal, M. Majumder and M. V. Shelke, *Materials Science and Engineering: B*, 2017, **223**, 24-34.

12. T. Alamro and M. K. Ram, *Electrochim. Acta*, 2017, **235**, 623-631.